Unraveling Dispersed Kinetic Behavior:
Dichlorofluorescein Isolated in Potassium Hydrogen Phthalate

1.1

Eric D Bott Erin A Riley Bart Kahr Phillip J Reid

Spectral Diffusion

We explored the role of spectral diffusion in the blinking dynamics of single DCF molecules in potassium acid phthalate (KAP) crystals. The emission from individual molecules was separated into spectral components using a dichroic mirror centered at 540 nm, then focused onto two avalanche photodiodes. This approach allowed us to monitor changes in emission energy from one molecule to another, as well as time-dependent spectral fluctuations (spectral diffusion) is a single molecule.

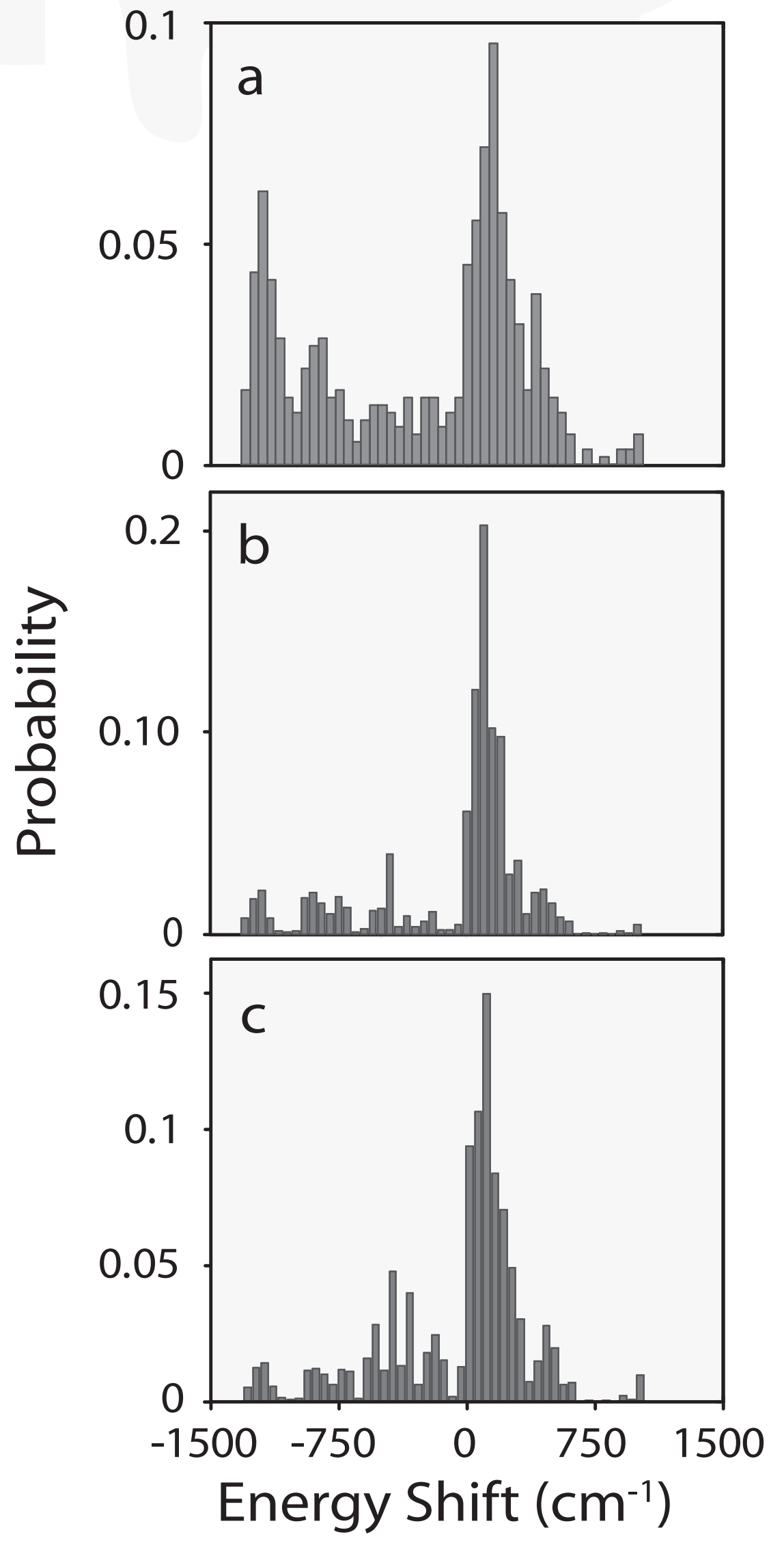

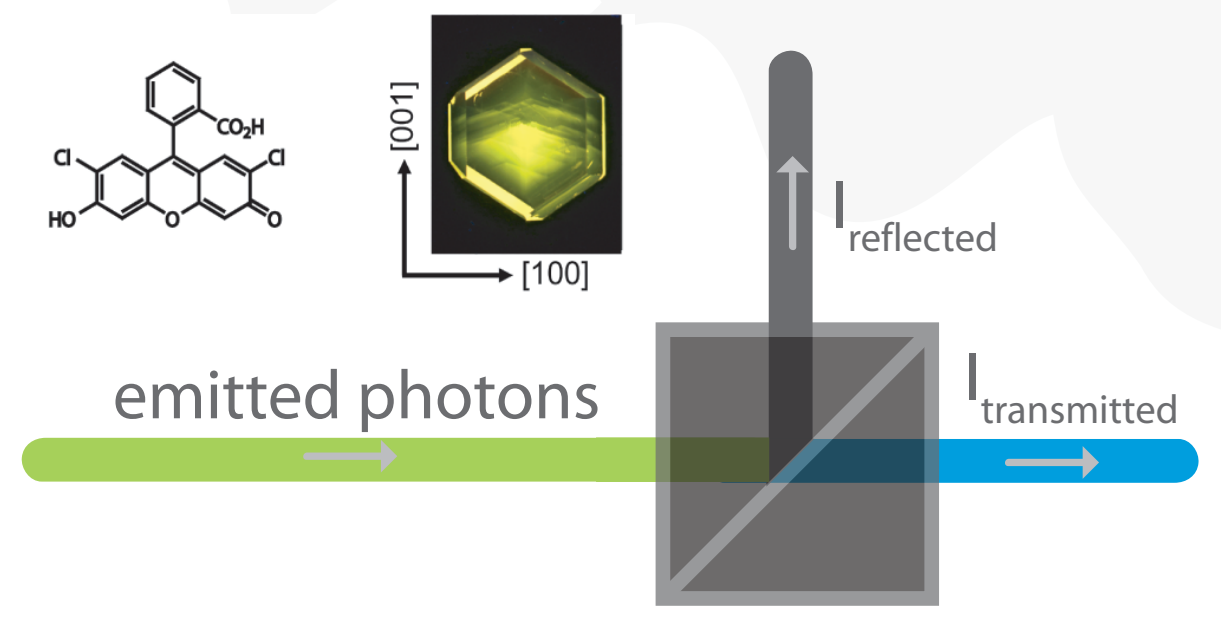

$$\langle R(t)\rangle = \langle I_{reflected} / I_{transmitted} \rangle$$

The combined intensity for each blinking trace was deconvolved using a change-point detection algorithm, the spectral energy shifts were calculated for every deconvolved segment based upon the average intensity ratio between the detectors. Histograms of energy-shift occurrences are shown left. The energy distribution in (a) is unweighted, (b) is weighted by segment duration to create a temporal-probability distribution of energy shifts. Panel (c) was calculated by using the total number of photons emitted from each occurrence shown in (a). This distribution best corresponds to the ensemble fluorescence.

The ensemble fluorescence maximum of DCF differs by roughly 1300 cm-1 between polar-aprotic and aqueous solutions (where the anionic form is dominant) and the same separation is evident in the segment-weighted energy-shift histogram, consistent with both forms in KAP at the SM level. Photo-induced proton transfer mechanisms may promote interchange between populations with different molar extinction coefficients, the etiology for intensity fluctuations and long lived dark states. The ability to extrapolate our mechanistic understanding fluorescence dispersion to molecular blinking is an attractive pursuit.

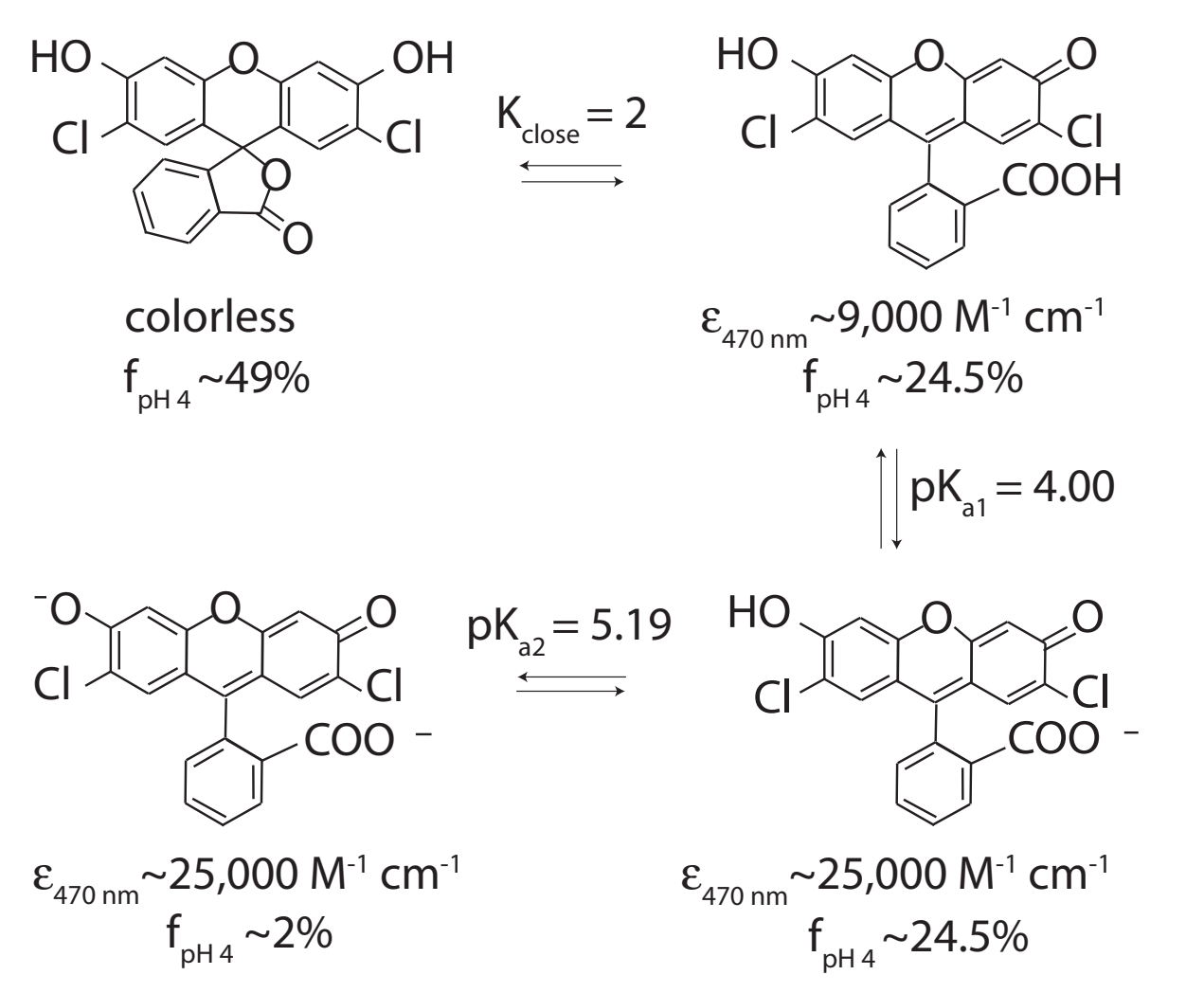

The different protonation forms of DCF with partition coefficients and estimated molar absorptivities at 470 nm at pH = 4. Clockwise, from top left, is the lactone, quinonoid, anionic and dianionic forms.

Intensity-Lifetime Analysis

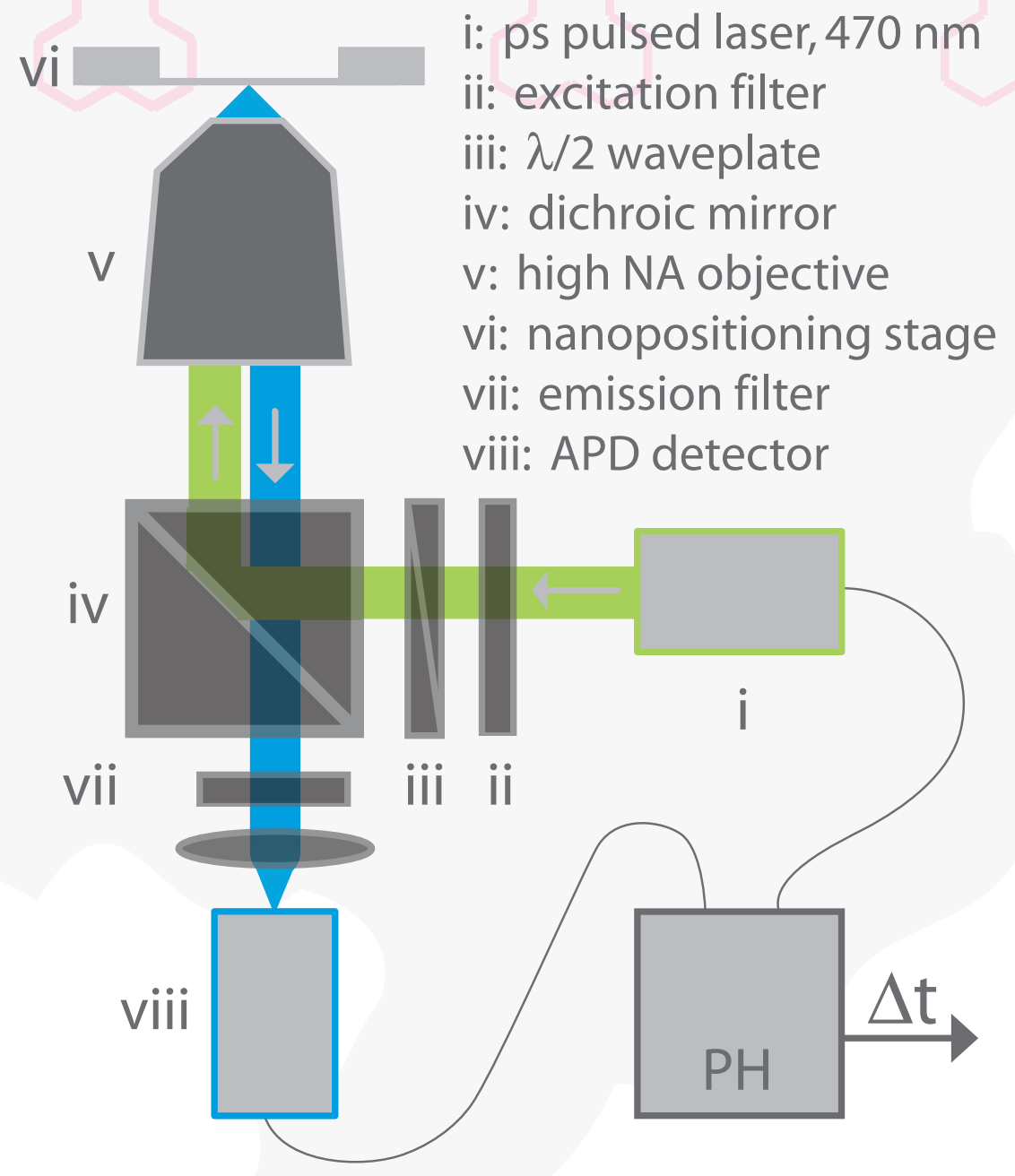

i: ps pulsed laser, 470 nm
ii: excitation filter
iii: λ/2 waveplate
iv: dichroic mirror
v: high NA objective
vi: nanopositioning stage
vii: emission filter
viii: APD detector

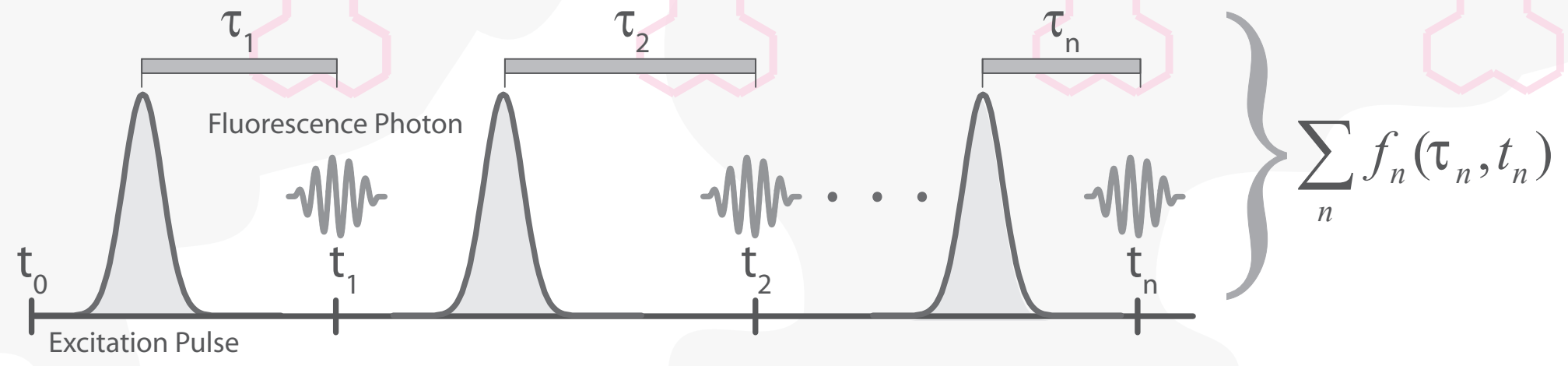

$$\sum_n f_n(\tau_n, t_n)$$

Blinking mechanisms were further explored with time-tagged time-resolved time-correlated single-photon counting (T3R-TCSPC), a technique capable of correlating single-molecule blinking dynamics, excited-state lifetimes, emission dichroism, and spectral profiles. In this technique, standard blinking traces are collected in addition to the temporal delay between each excitation pulse (τ_n) and when a emissive photon is detected (t_n).

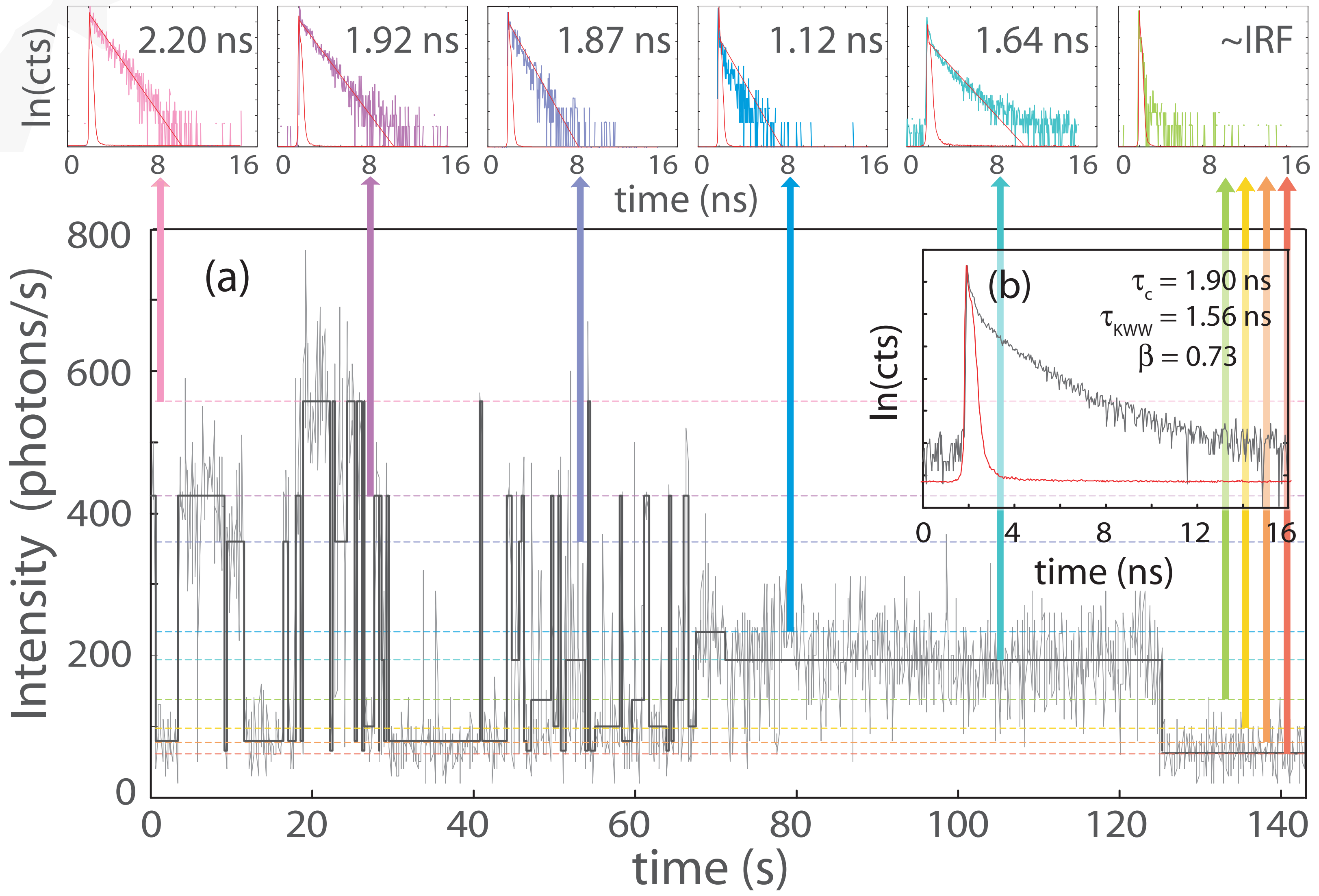

A T3R-TCSPC trace for DCF in KAP is shown above, with a blinking trace (grey line) and the emissive states as determined by change-point-detection analysis is shown (black line). Above are represented the lifetime decays for each intensity state. The excited state lifetimes determined for segments of same intensity level are equivalent even though the segments occur at different times in the trace. This observation demonstrates that the excited-state lifetime of a given intensity state is the same irrespective of when the state is populated, though the convolution of all decay events for an entire trace exhibits a stretched-exponential decay (b). 46 molecules of 61 had overall lifetime decays that were stretched exponential, while the remaining 15 exhibited single-exponential overall decays.

The distribution of excited-state lifetimes for all 61 DCF molecules in KAP is shown in (a), right. The lifetimes span 0.6 to 7.8 ns, with an average of 3.02 ± 1.8 ns. (b) presents excited-state lifetimes for the molecules that exhibited single-exponential excited-state decay, and (c) the lifetimes for molecules that exhibited stretched-exponential excited-state decay. Molecules exhibiting single-exponential decay have a narrow distribution of lifetimes, and the corresponding distribution for molecules exhibiting stretched-exponential decay is significantly broader. This data was further explored using intensity-lifetime analysis (ILA). In ILA, the intensities observed in a trace are normalized with respect to the highest-intensity observed during the trace. Then the excited-state lifetime for each state is normalized relative to the corresponding lifetime for the highest-intensity state. The idealized ILA scatter (lower right), demonstrates how each area represents the extent of radiative (Δk_{rad}) and non-radiative (Δk_{nr}) rate constant modification, as well as the extent of spectral diffusion (ΔA).

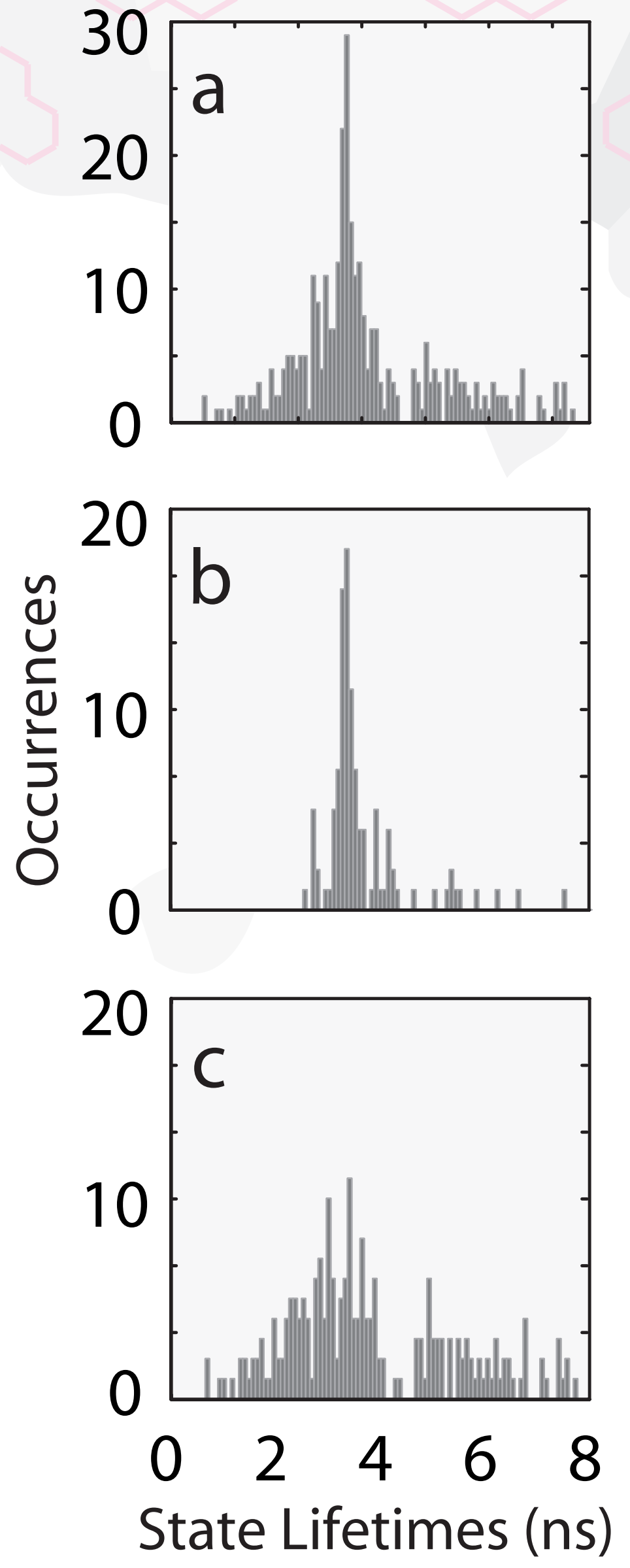

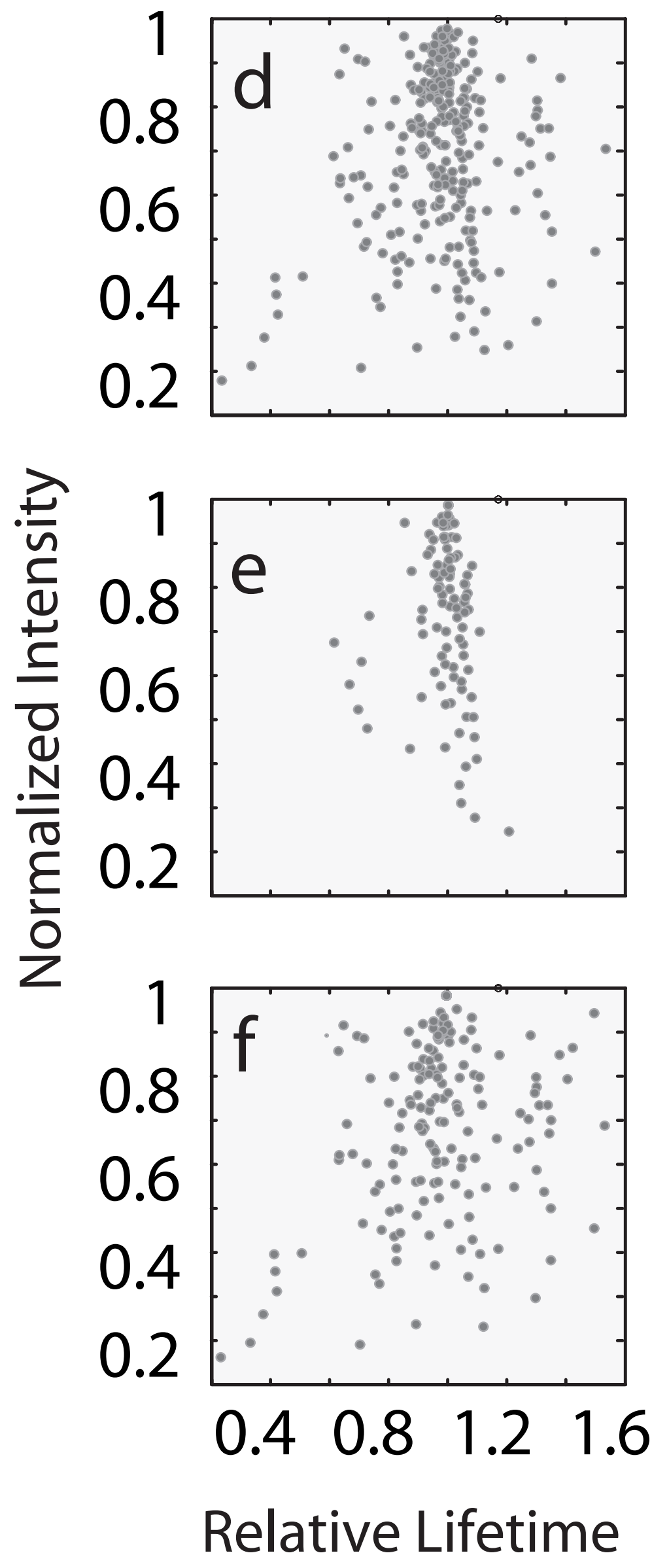

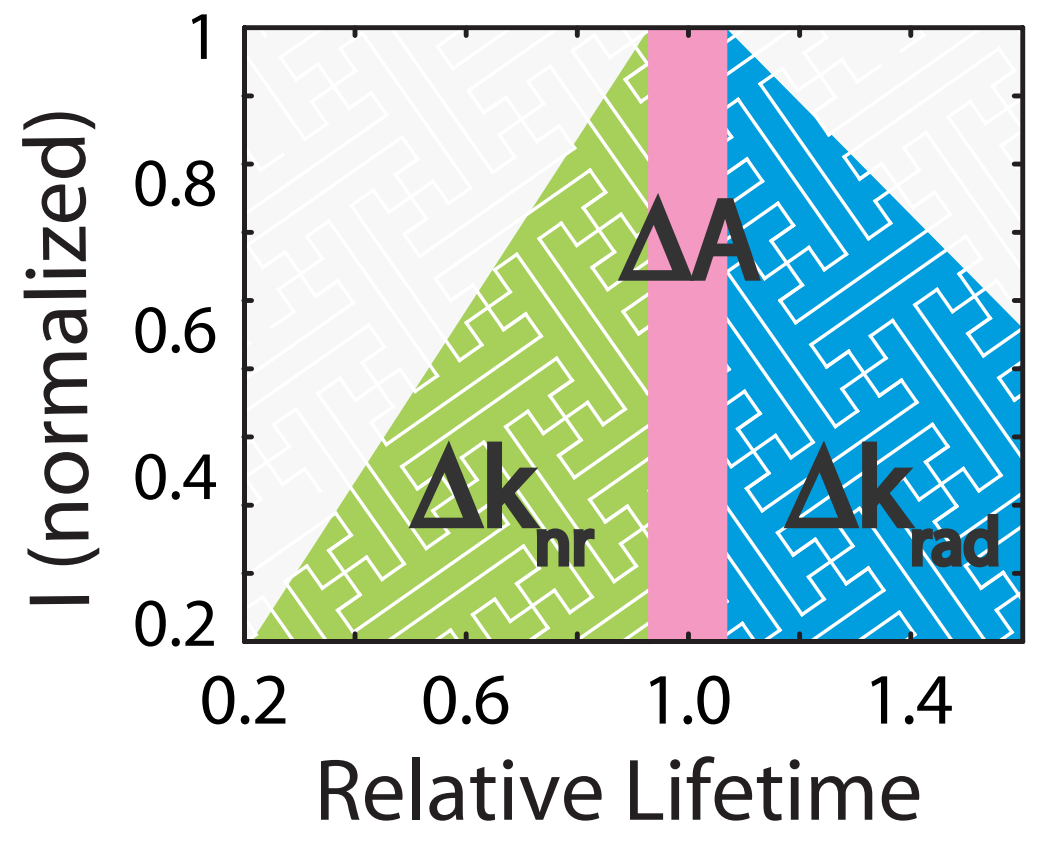

Panels d-f, left, present the resulting ILA plots for all molecules (d), molecules demonstrating single-exponential decay (e), and those demonstrating stretched-exponential decay (f). The correlation plot for all molecules demonstrates a high degree of dispersion, however decomposition of these data into molecules exhibiting single-exponential (5e) and stretched-exponential decay (5f) reveals that the stretch-exponential population is largely responsible this dispersion. These results show that intensity modification of SMs is complex, and could arise from changes in the protonation state of DCF in KAP.

NSF MDITR UNIVERSITY OF WASHINGTON